# Transport properties of molten alkali halides

G. Ciccotti* and G. Jacucci
*Centre Européen de Calcul Atomique et Moléculaire, Faculté des Sciences, 91405 Orsay, France and G.N.S.M., Consiglio Nazionale delle Richerche, Istituto di Fisica, Università di Roma, Rome, Italy*

I. R. McDonald
*Department of Chemistry, Royal Holloway College, Egham, Surrey, England*
(Received 14 May 1975)

The transport properties of molten alkali halides have been calculated in molecular dynamics "experiments" based on rigid-ion pair potentials of the Huggins-Mayer form with parameters proposed by Tosi and Fumi. The coefficients of shear viscosity and electrical conductivity are obtained by computing the response of the system to a small applied field of the appropriate type, and the extension of the method to the calculation of current-current correlation functions of acoustic and optic character is also considered. Comparison with experimental data shows that the electrical conductivities are very well reproduced, but systematic discrepancies are found for diffusion coefficients and viscosities.

## I. INTRODUCTION

A number of papers[1-3] have now appeared in which the thermodynamic properties of molten alkali halides have been studied in computer "experiments," but relatively little work on the dynamical properties has so far been reported. In the present paper we describe the results of a series of molecular dynamics calculations of the transport coefficients and collective dynamical modes of a selected group of salts at temperatures close to the respective triple points: LiF, NaCl, NaI, KI, RbCl, and RbI. In all cases we adopt the rigid-ion potentials proposed by Tosi and Fumi,[4] and one of our main objectives is to assess how far it is possible to describe the transport properties of such systems without allowing for the effects of polarization.

No theory exists which makes it possible to relate the various features of transport in molten salts to the different terms in the potential, and rather little is known about the importance to be attached to differences in mass and size and to ionic polarizability. In pure atomic fluids, where the mass appears as a scaling factor of the time, the geometrical factor can be accounted for on the basis of a hard-sphere model,[5,6] dispersion forces playing only a minor role. In binary mixtures, even of simple liquids such as the rare gases, the problem is more complicated, and here computer simulation helps in establishing empirical correlations. It has been shown,[7] for example, that diffusion in mixtures depends on the atomic packing in much the same way as in pure fluids. In ionic melts an added difficulty is the presence of the long-range Coulomb interaction, which contributes most of the potential energy of the system. Furthermore, the effects of polarization cannot be taken into account in any simple way.

From the remarks we have made it is clear that we do not expect to be able to interpret our results in terms of the detailed character of the individual ions. What we are more concerned with is an examination of the extent to which the transport properties of molten salts can be described on the basis of potentials which have been fitted to experimental equilibrium data, no explicit reference being made to the question of polarization. It might be expected that polarization would facilitate the process of diffusion because the screening of the ion which is diffusing can be provided by a polarization cloud; in a rigid-ion model the maintenance of local charge neutrality can be achieved only by bodily displacement of the ions. Another phenomenon in which polarization may play a part is that of correlated motion of ions of opposite charge. Correlations of this type alter the relative contributions made to diffusion and electrical conductivity and are responsible for the observed deviations from the Nernst-Einstein relation.[8]

Much is still unknown about the collective dynamical properties of molten salts, and computer experiments have an important role to play here. Questions such as whether the characteristic frequencies of transverse and longitudinal modes of acoustic and optic character are drastically reduced upon melting, or that of determining the range of the wave vector in which propagating modes exist, have so far been answered only partially or not at all. These particular collective modes are in any case clearly separable only in the long-wavelength limit, and a topic of considerable interest in itself[9] is that of constructing a set of orthogonal dynamical variables which can be used to describe the dynamical properties of the melt over the range of wave vectors from the

hydrodynamic regime to the merging into free-particle modes.

The computational effort necessary to obtain accurate values for transport coefficients by the usual means is rather heavy. To overcome this problem we have exploited the method described elsewhere,[10] in which the response of the system to a small perturbation is calculated directly. In this way we have computed the current-current correlation functions at several wave vectors, and from these we have evaluated the coefficients of electrical conductivity and shear viscosity. The conductivity is obtained from the transverse optic current autocorrelation function, and the viscosity is calculated by extrapolation to zero wave vector of the integral of the transverse acoustic correlation function. We have also obtained some information on the small cross-correlations between acoustic and optic modes. Finally, for each species $\alpha$ we have evaluated the diffusion coefficient $D_\alpha$ from the usual formula

$$D_\alpha = \frac{k_B T}{m_\alpha} \int_0^\infty Z_\alpha(t)\, dt, \tag{1}$$

where $Z_\alpha(t)$ is the normalized velocity autocorrelation function

$$Z_\alpha(t) = \langle \vec{v}_{i\alpha}(t) \cdot \vec{v}_{i\alpha}(0) \rangle / \langle |\vec{v}_{i\alpha}|^2 \rangle . \tag{2}$$

## II. METHOD OF CALCULATION

### A. Molecular dynamics

We have closely followed the methods used in other[8,11] molecular dynamics "experiments" on Coulombic systems. All calculations were made for systems of 216 ions, with periodic boundary conditions, and the electrostatic energy was evaluated by the Ewald method.[12] The potential used was of the generalized Huggins-Mayer form proposed by Tosi and Fumi,[4] which we may write as

$$\varphi(r_{ij}) = \frac{Q_i Q_j}{r_{ij}} + b c_{ij} \exp[(a_i + a_j - r_{ij})/\lambda] - \frac{C_{ij}}{r_{ij}^6} - \frac{D_{ij}}{r_{ij}^8}, \tag{3}$$

where $Q_i$ and $Q_j$ are the ionic charges. The terms on the right-hand side of Eq. (3) represent, successively, the Coulombic interaction, overlap repulsion, and dipole-dipole and dipole-quadrupole dispersion forces. The values used for the various parameters in the potential (3) are listed in Table I.

The thermodynamic states studied are summarized in Table II, together with some other relevant information; $\Delta t$ is the time step in the numerical integration of the equations of motion and $N_t$ is the total number of integration steps. The temperature is in all cases some 5% higher than that of the corresponding triple point.

All the molecular dynamics runs were broken up into what we call "segments," typically lasting for 60 time steps. The trajectories of the ions in each segment were computed twice, starting from the same initial configuration. In one case the calculation proceeded in the normal way; in the other, one or more small forces, of order 1 eV cm$^{-1}$, were applied to the ions. The currents induced in the system by the action of the applied force were computed as functions of time simply by calculating the *difference* in current in the perturbed and unperturbed trajectories, and were averaged over all segments making up the run. By a standard result of linear response theory,[13] the *mean* induced current can be related to the autocorrelation function of the appropriate dynamical variable. Specifically, if $\Delta B(t)$ is the change induced in a variable $B$ by an external potential $\varphi_A$ which is conjugate to a variable $A$, then in the mean we can write

$$\langle \Delta B(t) \rangle = \frac{1}{k_B T} \int_{-\infty}^{t} \langle \dot{A}(0) B(\tau) \rangle \varphi_A(\tau)\, d\tau . \tag{4}$$

The basis of the method has been discussed elsewhere.[10] Here we restrict ourselves to a consideration of the particular problems which arise in the case of molten salts, formal details being given in the Appendix.

Note that the number of time steps quoted in Table I refers to the number of *independent* con-

TABLE I. Parameters in the interionic potentials. $b = 3.38 \times 10^{-13}$ erg; $c_{++} = 1.25$ (2.0 for LiF), $c_{+-} = 1.0$ (1.375 for LiF), and $c_{--} = 0.75$.

| Salt | $a_+$ (Å) | $a_-$ (Å) | $\lambda$ (Å) | $C_{++}$ | $C_{--}$ | $C_{+-}$ | $D_{++}$ | $D_{--}$ | $D_{+-}$ |
|---|---|---|---|---|---|---|---|---|---|
| | | | | ($10^{-60}$ erg cm$^6$) | | | ($10^{-76}$ erg cm$^8$) | | |
| LiF | 0.816 | 1.179 | 0.299 | 0.073 | 14.5 | 0.8 | 0.03 | 17 | 0.6 |
| NaCl | 1.170 | 1.585 | 0.317 | 1.68 | 116 | 11.2 | 0.8 | 233 | 13.9 |
| NaI | 1.170 | 1.907 | 0.386 | 1.68 | 392 | 19.1 | 0.8 | 1100 | 31 |
| KI | 1.463 | 1.907 | 0.355 | 24.3 | 403 | 82 | 24 | 1130 | 156 |
| RbCl | 1.587 | 1.585 | 0.318 | 59.4 | 130 | 79 | 82 | 260 | 134 |
| RbI | 1.587 | 1.907 | 0.337 | 59.4 | 428 | 135 | 82 | 1200 | 280 |

TABLE II. Results of molecular dynamics calculations. Values in parentheses are experimental results.

| Salt | $\Delta t$ ($10^{-14}$ sec) | $N_t$ ($10^3$) | $V$ ($cm^3\,mol^{-1}$) | $T$ (K) | $D_+$ ($10^{-5}\,cm^2\,sec^{-1}$) | $D_-$ | $\sigma$ (mho $cm^{-1}$) | $\eta$ (cP) | $\Delta$ | $S$ |
|---|---|---|---|---|---|---|---|---|---|---|
| LiF | 0.4 | 5.0 | 15.00 | 1287 | 13.6 | 11.3 | 12.1 (9.3) | 1.14 | 0.16 | 0.159 |
| NaCl | 0.8 | 7.5 | 39.10 | 1262 | 10.6 (14.0) | 9.9 (10.1) | 4.2 (4.2) | 0.87 (0.83) | 0.09 (0.18) | 0.141 |
| NaI | 1.2 | 5.0 | 57.46 | 1081 | 9.4 (10.5) | 6.8 (5.9) | 2.5 (2.7) | 1.08 (1.01) | 0.14 (0.08) | 0.180 |
| KI | 1.8 | 8.5 | 68.97 | 989 | 4.5 | 3.7 | 1.42 (1.38) | 1.06 (1.40) | −0.06 | 0.107 |
| RbCl | 1.2 | 5.0 | 56.48 | 1119 | 5.0 (6.6) | 5.2 (5.8) | 1.81 (1.81) | 0.99 (0.90) | −0.01 (0.15) | 0.104 |
| RbI | 1.6 | 5.0 | 75.75 | 1086 | 4.3 | 3.5 | 1.09 (1.09) | 1.12 (0.96) | −0.03 | 0.102 |

figurations. The total number of configurations generated for each system was $2N_t$, half in the perturbed and half in the unperturbed trajectory. The unperturbed trajectories were all continuous, one segment leading directly onto the next.

### B. Electrical conductivity

A simple example of the use of the method is the application to electrical conductivity. In this case the force acting on an ion $i$ located at $r_i$ is taken to be

$$\vec{F}(\vec{r}_i, t) = F_x(Q_i/e)\theta(t)\vec{x}, \tag{5}$$

where $\vec{x}$ is a unit vector in the $x$ direction and $\theta(t)$ is the step function

$$\theta(t) = 0, \quad t < 0, \qquad = 1, \quad t > 0. \tag{6}$$

The response which is computed is the induced electrical current in the same direction

$$J_x^Q(t) = \sum_i Q_i v_{ix}(t). \tag{7}$$

The electrical conductance can be calculated from the statistical average of $J_x^Q(t)$ in the limit $t \to \infty$, obtained as a difference between perturbed and unperturbed trajectories. It follows that the segment must be sufficiently long for $J_x^Q(t)$ to attain a plateau value. Application of Eq. (4) shows that the response is related to spontaneous fluctuations in the unperturbed system by

$$\langle J_x^Q(t)\rangle = \frac{1}{ek_BT}\int_0^t \langle J_x^Q(0)J_x^Q(\tau)\rangle F_x\,d\tau. \tag{8}$$

In other words, the mean response is proportional to the time integral of the autocorrelation function of the electrical current.

The matrix of electrical current correlation functions is diagonal in homogeneous systems, and in the statistical mean only the $x$ component of the induced current remains. The mechanical response function does not have the same property, and there will be a random response in directions orthogonal to the applied force which will depend on the initial conditions. In Fig. 1(a) we show a graph of $\langle J_x^Q(t)\rangle$ as a function of $t$ in the case of RbI, obtained by averaging over 60 segments. We also plot the mean current in the orthogonal directions, which we take as a guide to the statistical error in the mean response. At short times the response grows linearly with a slope determined by the ionic masses. It later passes through a maximum and then attains a constant level. It is of course essential that the plateau value is reached before the noise becomes unacceptably large. Finally, the specific conductivity is given by

$$\sigma = e\langle J_x^Q(\infty)\rangle / VF_x, \tag{9}$$

where $V$ is the volume of the molecular dynamics cube.

It is obvious from the fact that both the perturbation and the response are independent of position in space that we are dealing with a current component of zero wave vector. In the $k \to 0$ limit it is not possible, *a priori*, to distinguish between longitudinal and transverse modes. However, the zero-$k$ limits of the two optic modes are quite distinct, their characteristic frequencies differing by the plasma frequency. For the reasons we recall below, the longitudinal-optic mode $k = 0$ cannot be observed in a computer "experiment," and the current we compute corresponds to the trans-

verse mode.

In a transverse-optic mode the charges of opposite sign oscillate in opposite phase with a displacement which varies along the direction of propagation of the wave. No charge accumulation results as a consequence of this motion and the restoring force has only a local origin. In a longitudinal-optic mode, however, the charges oscillate in the direction of the wave vector, the magnitude of displacement again varying along the direction of propagation. This does lead to charge accumulation, as can be seen by focusing attention on the nodes of the waves, where the displacements change sign. The nodal planes are accumulation regions for alternately positive and negative charges, and it is clear that the origin of the additional restoring force that raises the longitudinal frequency above the transverse one by a value equal to the plasma frequency is just the Coulomb interaction between these rather distant charge distributions. This effect is present, no matter how long the wavelength, because of the infinite range of the Coulomb potential. It is then obvious that in order to take correctly the limit $k \to 0$ it is necessary to work with a system which contains a full period of the longitudinal oscillation, thereby ensuring that the attraction between the charge distributions accumulated on adjacent nodal planes is taken into account. If this is not done, it is not to be expected that the optical oscillation of the system will be speeded up by the extra restoring force related to the plasma oscillation. In molecular dynamics, however, the limit $k \to 0$ is by necessity taken on a local basis, that is, by monitoring a finite portion of the system *within* the infinite wavelength.

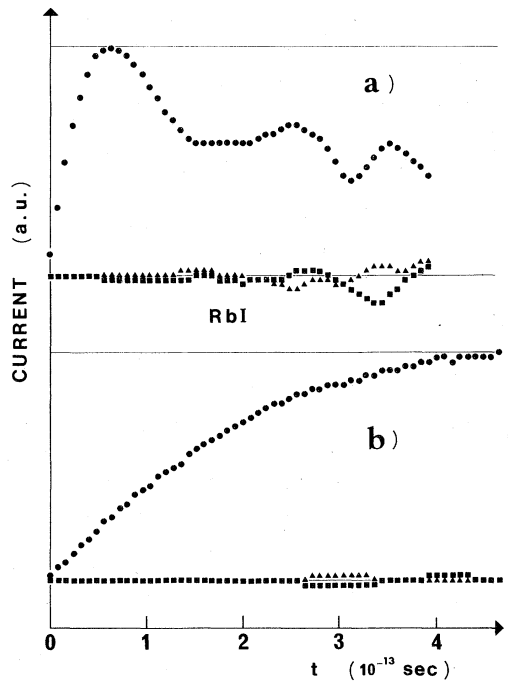


FIG. 1. Computed response in arbitrary units in the calculation of (a) electrical conductivity, and (b) shear viscosity of RbI.

A last remark on the calculation of conductivity has to do with macroscopic polarization. The forces we apply act directly on the ions; there are no surfaces on which charges accumulate, and the electric current flows in the closed toroidal surface generated by the periodic boundary condition. Consequently, the number we compute is the internal or local conductivity.

### C. Shear viscosity

The evaluation of the shear viscosity is carried out by applying a shearing force which is periodic in space and has by necessity a finite wave vector,

$$\vec{F}(\vec{r}_i, t) = \mathrm{Re} F_x e^{i\vec{k}\cdot\vec{r}_i}\,\theta(t)\vec{x}. \tag{10}$$

We assume that the force $\vec{F}$, which by construction is orthogonal to $\vec{k}$, is directed along the $x$ axis.

This is the same type of perturbation as that used by Gosling *et al.*[14] in computing the shear viscosity of argonlike liquids. The response we compute is the $k$th Fourier component of the drift velocity $\langle \hat{u}_x(\vec{k}, t)\rangle$. A straightforward hydrodynamic calculation shows that the limiting value of this quantity, which turns out to be the same for each species, is related to the shear viscosity $\eta$ by

$$\eta = \lim_{k\to 0} \frac{\rho F_x}{k^2 \langle \hat{u}_x(\vec{k}, \infty)\rangle}, \tag{11}$$

where $\rho$ is the number density. The long-wavelength limit in Eq. (11) is taken by computing the response to the perturbations having the two smallest wave vectors which are accessible in our periodic system, $\vec{k} = (2\pi/L)(0, 0, 1)$ and $\vec{k} = (2\pi/L)(0, 1, 1)$, where $L$ is the length of the cube, and then extrapolating linearly in $k^2$ to $k = 0$. (The term in $k$ must vanish on grounds of symmetry.) At short times the slope of the response $\langle \hat{u}_x(\vec{k}, t)\rangle$ as function of $t$ is different for the two species and depends upon the mass.

As a variation on Eq. (10) we can choose to apply forces of different intensity to the ions of different species. A particularly simple choice is one in which the force is proportional to the mass, in which case the accelerations are the same. The limiting drift velocities of the two species again turn out to be equal to each other and equal to that attained in the previous case, provided the magnitude of the forces is adjusted in such a way as to leave unaltered the total body force acting

on a given configuration. We interpret this as implying that there is a unique shear viscosity in mixtures, regardless of whether the flux is sustained by gravity or by pressure. In the case when the mass-weighted perturbation is applied, the mean response is proportional to the integral of the transverse mass-current autocorrelation function. The demonstration of this equivalence is given in detail in the Appendix.

The mean response to a perturbation of the form of (10) is plotted as a function of $t$ in Fig. 1(b), again for the case of RbI. The behavior is very different from that obtained in the calculation of conductivity, the plateau value being reached asymptotically. Furthermore, the noise level is much smaller, even though the average was computed over 30 segments rather than 60. The reason is simply that in a long-wavelength acoustic-type perturbation the forces on neighboring ions are nearly in phase, whereas in an optic-type perturbation such as (5) the forces on neighboring ions of opposite sign push such ions towards each other. The random response is therefore greater in the second case.

### D. Current-current autocorrelation functions

It should be clear from the discussion given in Secs. II B and II C that the techniques used for the evaluation of conductivity and shear viscosity are special cases of the calculation of correlations in the wave-number–dependent fluctuations in the currents of charge and mass. For KI and NaCl we have used a more general approach to obtain information on the collective modes for selected values of the reduced wave number $n$, where $k = n(2\pi/L)$. We apply a force in the $x$ direction, say, with a magnitude which varies periodically in space in either the $x$ direction for longitudinal modes or in the $z$ direction for transverse modes. At any given point in space the applied force acts either (a) in the same sense on all ions but with a magnitude proportional to the mass, or (b) in opposite senses on ions of different charge but with equal magnitude. Case (a) corresponds to acoustic-type modes and gives rise to mass currents; case (b) corresponds to optic-type modes and gives rise to charge currents. A more detailed discussion is contained in the Appendix.

In these calculations the force was applied only at $t = 0$, so that the mean response at a later time is the autocorrelation function of the corresponding current rather than the integral. Strictly speaking, this statement is correct only when the force is a true $\delta$ function in time. In fact, because of the use of a finite time interval in the numerical integrations, the force actually applied is a finite pulse of width $\Delta t$, but for practical purposes the distinction is not important.

In this way we have computed the longitudinal L and transverse T components of the autocorrelation functions of mass $M$ and charge currents. These functions we denote, in an obvious notation, by $C^{L}_{MM}(k,t)$, $C^{T}_{MM}(k,t)$, $C^{L}_{QQ}(k,t)$, and $C^{T}_{QQ}(k,t)$. Note that the electrical conductivity is given by the integral of $C^{T}_{QQ}(0,t)$ and the shear viscosity by the integral of $C^{T}_{MM}(0,t)$. We have also measured the small cross correlations of longitudinal currents of mass and charge described by the function $C^{L}_{MQ}(k,t)$ by computing the optic response to an acoustic-type perturbation or vice versa.

The calculations of the current correlation functions were made by simultaneously applying a number of perturbations. This has the effect of increasing the random response; in order to reduce the resulting noise level, the statistical averages were computed over 100 segments.

## III. RESULTS AND DISCUSSION

### A. Transport coefficients

The calculated values of the transport coefficients are listed in Table II together with the experimental results, where these are available. We estimate the statistical uncertainties in the molecular dynamics calculations to be approximately 3% in $D_+$ and $D_-$ and 5% in $\sigma$ and $\eta$. The experimental data are taken from the work of Young and O'Connell.[15] These authors have presented an empirical corresponding-states correlation of the transport coefficients of 1:1 alkali-metal molten salts. In some cases we have been obliged to make a small interpolation of their results, but we do not believe that any significant error has thereby been introduced.

In Fig. 2 we show some representative velocity autocorrelation functions. When one ion is significantly smaller than its partner, the corresponding autocorrelation function is strongly oscillatory. When the ions are approximately equal in mass, however, the two autocorrelation functions not only resemble each other but also are not very different from that of an argonlike liquid near its triple point. This second similarity is illustrated very well by the simplest case when both mass and size are equal, as in the system studied by Hansen and McDonald.[8] The oscillations which are seen when the ionic sizes are significantly different are considerably more pronounced than those observed,[7] say, in mixtures of Lennard-Jones fluids. Presumably the effect of the Coulombic force is to accentuate those features of the autocorrelation which originate in differences

in mass and size. On the other hand, we do not believe that the behavior we observe is related to the strong plasma-type oscillation which characterizes[11] the velocity autocorrelation function of the classical one-component plasma (OCP). Oscillations occur in the case of the OCP because of a coupling between the motion of single particles and the propagating density fluctuations which in that system coincide with the fluctuations in charge. The equivalent mechanism in a molten salt would be a coupling between single-particle and collective optic-type modes; there is no evidence to suggest that any such effect is present.

Of the six salts for which we have made calculations, diffusion coefficients are available only for NaCl, NaI, and RbCl. In all cases except one ($I^-$ in NaI) the computed value is too small, and the discrepancies are considerably larger for the metal ions than for the halogens.

It is tempting to look for some systematic effect of substitution of ions in different salts. Let us consider the following four systems: NaCl, NaI, RbCl, and RbI. For these we find values of the ratio $D_+/D_-$ equal to 1.07, 1.38, 0.96, and 1.23, respectively. If we now take the ratio of the second of these numbers to the first and of the fourth to the third we obtain the ratio of the diffusion constant of $Cl^-$ to that of $I^-$ in $Na^+$ and $Rb^+$ salts. The two numbers we find are 1.29 and 1.28, respectively. On the other hand, if we take the ratio of first to third and second to fourth in the list of values of $D_+/D_-$ we obtain the ratio of the diffusion constant of $Na^+$ to $Rb^+$ in $Cl^-$ and $I^-$ salts. We now find values of 1.11 and 1.12, respectively. The near equality of the two values in each case is presumably not accidental, but we have been unable to relate the numbers to any microscopic parameters such as mass or ionic radius.

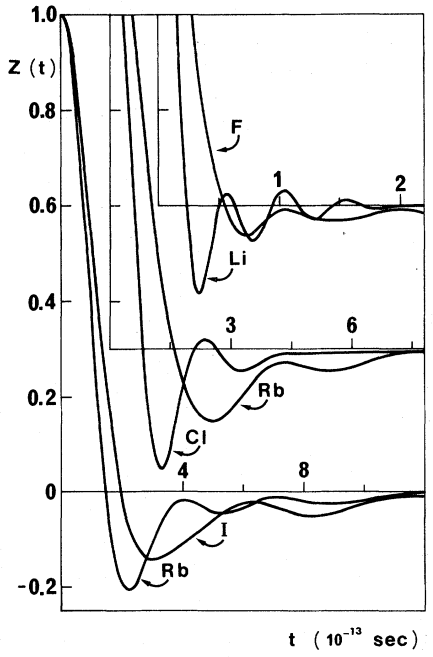


FIG. 2. Velocity autocorrelation functions for LiF, RbCl, and RbI.

Experimental data on electrical conductivity are available for all the salts we have studied. Agreement is remarkably good, except for LiF, for which there is a discrepancy of more than 20%. There is also some disagreement in the case of NaI, but for the other systems the discrepancies are less than the statistical error in the calculation. This clearly implies that electrical conductivity is not a quantity that is sensitive to details of the potential, and is almost entirely determined by the masses and diameters of the ions. Furthermore, polarization presumably makes only a very small contribution. (Polarization is unlikely to play any significant role in LiF, where the largest discrepancy is found.)

The electrical conductivity may be related to the mean diffusion constant through the Nernst-Einstein relation

$$\sigma = \tfrac{1}{2}(Ne^2/Vk_BT)(D_+ + D_-)(1-\Delta). \tag{12}$$

If cross-cross correlations of the type $\langle \vec{v}_i(0)\cdot\vec{v}_j(t)\rangle$ $(i \neq j)$ made no net contribution to the autocorrelation of the electrical current, then the deviation $\Delta$ would be zero. There is no such contribution to the interdiffusion current in the case of mixtures of rare-gas liquids; the mutual diffusion coefficient is very closely approximated by the appropriately weighted mean of the self-diffusion coefficents.[7] In molten salts there is a strong positive correlation in the velocities of neighboring ions of opposite charge, which in turn means that $\Delta$ is positive. Experimentally, $\Delta$ is of order 0.1–0.2 for the alkali halides and of order 0.3–0.4 for the alkali nitrates. Our results on $\Delta$, which are listed in Table II, are considerably smaller overall than the experimental results we have quoted. For the salts with lighter metal ions ($Li^+$ and $Na^+$) the deviation is positive but small; it is zero within the statistical error for $K^+$ and $Rb^+$ salts.

Experimental shear viscosities are available for all salts studied except LiF. Comparison between calculation and experiment reveals a broadly consistent pattern. If we exclude KI we see that the molecular dynamics result is systematically larger than the experimental one, the discrepancy lying everywhere between 5% and 10%. KI is an anomalous case; the experimental value is considerably larger than for any other molten salt, a

fact for which there is no obvious explanation, and the molecular dynamics result is 24% too small.

There is an additional source of uncertainty in the calculation of $\eta$, namely, the extrapolation to zero wave number which is required in Eq. (11). We have explicitly made the extrapolation in $k^2$, which we described earlier only for NaCl, for which an increase by a factor of 1.29 was found between the smallest $k$ value and $k=0$, and for NaI, for which the factor was 1.37. For the other salts we have used the mean of these two numbers, i.e., 1.33. In the case of NaCl we have made a more detailed study, extending the calculation of the drift velocity to higher $k$ values, and have found a rather complicated nonlinear behavior in $k^2$. This is a point which merits further attention.

Alder *et al.*[16] have shown by molecular dynamics that the diffusion coefficient and shear viscosity of the hard-sphere fluid are accurately related through the Stokes relation, with a constant of proportionality appropriate to "slipping" boundary conditions. A similar correlation has also been shown to exist for the Lennard-Jones fluid.[5,14] The application of the Stokes relation to molten salts is of course a dubious procedure. If we adopt the model uncritically we expect to find the parameter $S$, given by

$$S=\tfrac{1}{2}\eta(D_+ +D_-)(a_+ +a_-)/k_BT, \qquad (13)$$

values lying between $1/3\pi=0.106$ ("sticking") and $1/2\pi=0.159$ ("slipping"). The results we obtain for $S$ are listed in Table II. We see that $S$ is indeed almost constant for the three salts in which the ions are most nearly equal in size (RbCl, RbI, and KI), but it rises rapidly as the size ratio increases (NaCl→ LiF→ NaI).

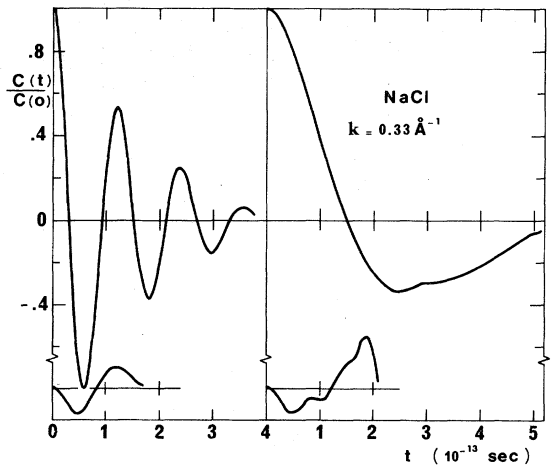


FIG. 3. Upper curves, longitudinal charge (left-hand side) and mass (right-hand side) current-current autocorrelation functions for NaCl at $k=0.33$ Å$^{-1}$. Lower curves are cross-correlation function $C^{L}_{MQ}(k,t)$ plotted on a vertical scale which has been increased by a factor of 7.

### B. Current-current autocorrelation functions

The correlation functions corresponding to longitudinal optic- and acoustic-type modes for the smallest accessible wave vector ($n=1$, $k=0.33$ Å$^{-1}$) in NaCl are shown in Fig. 3. The function $C^{L}_{QQ}(k,t)$ shows a very pronounced oscillation corresponding to a well-defined propagating charge fluctuation similar to that previously observed in a simpler system.[8] The function $C^{L}_{MM}(k,t)$ shows a much more strongly damped oscillation. The corresponding power spectra $C^{L}_{QQ}(k,\omega)$ and $C^{L}_{MM}(k,\omega)$ are plotted in Fig. 4. In each case there is a clearly defined peak, but if we divide $\omega^2$ in order to obtain the corresponding dynamical structure factors (shown as dashed lines on different relative scales) the acoustic peak disappears, whereas the optic peak suffers only a minor displacement towards lower frequencies. The peaks in the power spectra are at $\omega_{LO}=5.2\times10^{13}$ and $\omega_{LA}=0.90\times10^{13}$ rad sec$^{-1}$. The latter values correspond to a longitudinal sound velocity of $2.7\times10^5$ cm sec$^{-1}$, which is larger by a factor of approximately 1.6 than the ordinary velocity of sound in NaCl.[17] The characteristic frequencies $\omega_{LO}$ and $\omega_{LA}$ may be compared with the phonon frequencies for the smallest wave vector in the rigid-ion solid[18] at the melting point ($V=31.37$ cm$^3$ mol$^{-1}$, $T=1153$ K). For the latter we find $\omega_{LO}=5.1\times10^{13}$, $\omega_{LA}=1.2\times10^{13}$ rad sec$^{-1}$. Clearly the effects of melting are much larger for the acoustic mode than for the optic one. (It must be remembered that the phonon frequencies cor-

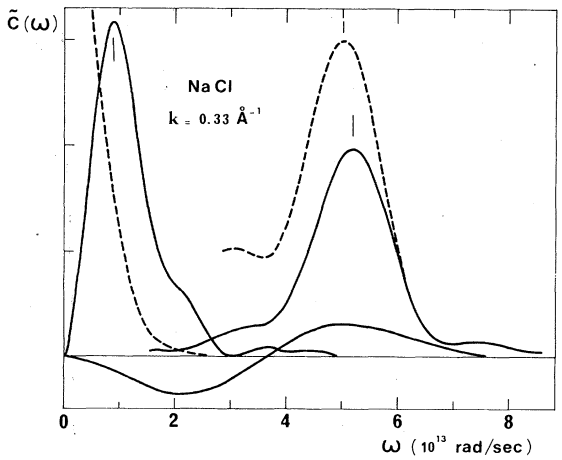


FIG. 4. Power spectra (full lines) of the autocorrelation functions shown in Fig. 3. The dashed lines are the result of dividing by $\omega^2$. Relative scales are arbitrary.

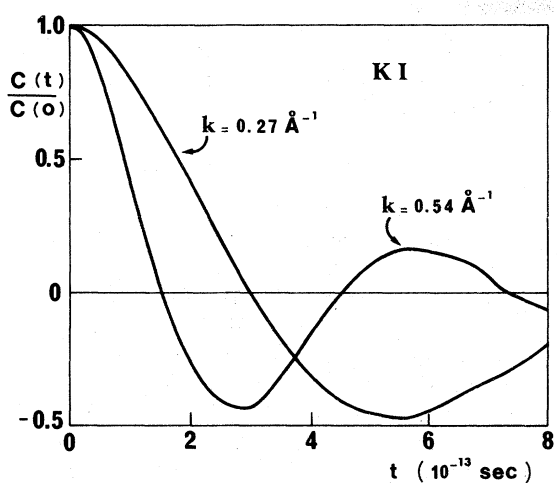


FIG. 5. Longitudinal mass current-current autocorrelation function for KI at $n=1$ ($k=0.27$ Å$^{-1}$) and $n=2$ ($k=0.54$ Å$^{-1}$).

respond to peaks in the dynamical structure factors.)

The second moments of the power spectra can be calculated from the short-time behavior of the correlation functions, which is particularly well-suited for study using the perturbation method. We find for the square roots of the moments $5.23\times10^{13}$ rad sec$^{-1}$ (optic) and $1.43\times10^{13}$ rad sec$^{-1}$ (acoustic). Thus the position of the optic peak coincides with the second moment of the distribution, but the acoustic peak shows a rather large shift.

In KI the two longitudinal autocorrelation functions for $n=1$ ($k=0.27$ Å$^{-1}$) behave very much in the same way as in NaCl. For $n=2$, however, the function $C^{L}_{MM}(k,t)$ still displays a full oscillation, whereas in NaCl the decay is overdamped. This behavior, illustrated in Fig. 5, suggests that a Brillouin peak may be more easily observed in KI.

In Fig. 6 we show the transverse acoustic correlation function in KI for $n=1$ and $n=3$. At the lower $k$ value the mode is purely diffusive and the power spectrum is centred at the origin. At $n=3$, however, there is an oscillatory behavior and a peak in the power spectrum is clearly visible, indicating the onset of propagating shear waves.

The transverse optic autocorrelation function at $k=0$ is shown in Fig. 7, again for KI. The interdiffusion correlation function is also plotted; the discrepancies between the two curves lie within the limits of statistical error. This figure justifies our association of the $k=0$ optical mode with the transverse charge current. For $n=3$ we find virtually an identical correlation function, whereas the longitudinal current correlation function is very different. We recall that in the solid there is a related result; the frequency of the transverse optic phonon is almost independent of $k$.

We now return our attention to Fig. 3. The small curves at the foot of the graph are the function $C^{L}_{MQ}(t)$, the measured cross correlation between acoustic and optic currents. This cross correlation is zero at $t=0$ and its maximum value is less than 1.5% of the zero-time value of the autocorrelation functions. (The scale of the cross-correlation function has been expanded by a factor of 7.) In the case shown the noise level is considerably higher when the cross correlation is measured as the optic response to an acoustic-type perturbation rather than vice versa, but we do not know whether this is true in general.

In Fig. 4 the long oscillation of low amplitude is the power spectrum $C^{L}_{MQ}(k,\omega)$, plotted on an arbitrary relative scale. The second moment of this spectrum is negative, as is obvious from the

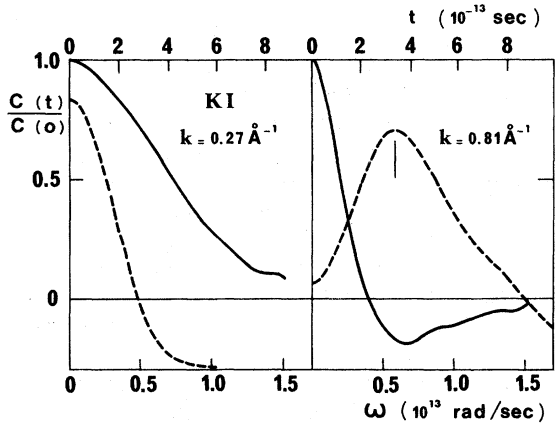


FIG. 6. Transverse mass current-current autocorrelation function for KI at $n=1$ ($k=0.27$ Å$^{-1}$) and $n=3$ ($k=0.81$ Å$^{-1}$). The dashed lines are the power spectra.

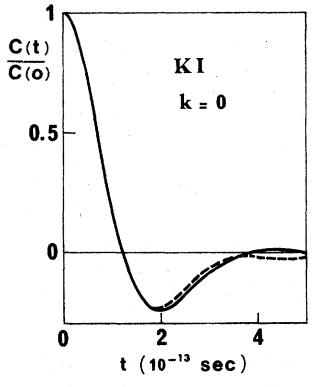


FIG. 7. Transverse charge current-current autocorrelation function for KI at $k=0$. The dashed line is the autocorrelation function of the electrical current.

shape of the corresponding time correlation function shown in Fig. 3.

The description of the collective modes of a molten salt in terms of mass and charge currents is in some respects not the best one. In particular, these variables are nearly independent only at long wavelengths. By an appropriate rotation of axes, however, it is possible to choose two linear combinations of currents which are more nearly orthogonal in the sense that the second moments of the cross-correlation function can be made to vanish at short times as well as at $t = 0$.[9] The hope in choosing such a transformation is that the corresponding dynamical structure factors will also be approximately diagonal, making it easier to describe the collective modes in terms of separable relaxation processes having different characteristic times. In practice, the resulting angle of rotation $\gamma$ turns out to be very small, at least at small $k$. For NaCl we find in the case of $n = 1$ that $\gamma = 0.7°$. For KI we find larger values, $\gamma = 1.8°$ for $n = 1$ and $\gamma = 9°$ for $n = 2$; apparently $\gamma$ increases rather rapidly with decreasing wavelength.

## IV. CONCLUSIONS

In the work described in this paper we have shown that the direct method of calculating time correlation functions can be successfully applied to a relatively complex system such as a molten salt, and detailed information on a variety of transport processes can be obtained with a comparatively modest computing effort. Our particular aim has been to investigate the extent to which a rigid-ion model can account for the transport coefficients of molten alkali halides. Anomalies exist, but the trends are largely systematic: The diffusion coefficients are underestimated, particularly that of the positive ion; the shear viscosity is overestimated, but only to a small extent; and the electrical conductivity is reproduced with remarkable accuracy. We have also gained some information on the collective modes of optic and acoustic character.

Some problems remain. In particular, we have not attempted any calculation of the thermal conductivity, and further development of the perturbation method in this direction is an obvious topic for future work. Furthermore, the method of computing the shear viscosity is not entirely satisfactory, because the extrapolation to zero wave number introduces some numerical uncertainty. It would be useful to find other quantities which also converge to the shear viscosity in the zero-$k$ limit but are less rapidly varying functions of $k$ at small $k$. For example, the stress tensor itself could be measured as a response to an applied field, and the advantages of studying this quantity should be investigated.

## ACKNOWLEDGMENTS

The bulk of this work was carried out during the course of the Centre Européen de Calcul Atomique et Moléculaire (CECAM) workshop on *Molecular dynamics of ionic systems* held at Orsay. We are grateful to Carl Moser, the director of CECAM, for making it possible for us to participate in this very successful meeting. We are also indebted to Eveline Gosling for the programming of the Ewald sums and to J. P. Hansen, A. Rahman, and K. Singer for useful discussions.

## APPENDIX

We give here the correlation-function formulas for the various currents induced in the system by external perturbations, presented in the general framework of the theory of the linear response of a system to an applied mechanical force which may or may not be derived from a potential. In particular, we will write the formulas quoted in the text for the electrical conductivity and the shear viscosity, and will formulate the general results of Kubo[13] and of Jackson and Mazur[19] in such a way as to permit the computation of the linear response of an observable to any applied longitudinal or transverse force field.

In essence, what these authors have proved by use of perturbation theory is that the variation in the statistical mean of any local dynamical variable $B(\vec{r}, t|\vec{r}_1, \ldots, \vec{r}_N; \vec{p}_1, \ldots, \vec{p}_N)$ in Fourier space is given by

$$\langle \Delta B(\vec{k}, \omega) \rangle = \sum_{j=1}^{3} \chi_{B,j}(\vec{k}, \omega) F_j^{\text{ext}}(k, \omega), \tag{A1}$$

where $\chi_{Bj}$ is a well-defined response function and $F_j^{\text{ext}}$ is the component of the external applied field in the direction $j$. The quantities $B(\vec{k}, \omega)$ of interest in the study of collective motions of many-body systems include the mass and number density, momentum and charge currents, microscopic stress tensor, heat-current density, and so on; therefore, we now adapt this result to the case of an arbitrary local tensorial variable of a two-component charged system, assuming that the change in the variable results from an applied mechanical force. For this purpose it is convenient to express any external field acting on a particle $i$ of mass $m_i$ as a linear combination of an optic-type and an acoustic-type field:

$$\vec{F}(\vec{r}_i, t) = \lambda_Q \vec{F}^Q(\vec{r}_i, t) + \lambda_M \vec{F}^M(\vec{r}_i, t), \tag{A2}$$

with

$$\vec{F}^{\alpha}(\vec{r}_i, t) = \alpha_i \vec{F}(\vec{r}_i, t) \tag{A3}$$

where

$\alpha_i = Q_i/e$ for $\alpha = Q$ (optic case),

$\alpha_i = Nm_i \Big/ \sum_{i=1}^{N} m_i$ for $\alpha = M$ (acoustic case).

It is well known that if $T(\vec{r}, t)$ is any local observable (in the general case a component of a tensor) such that at equilibrium $\langle T(\vec{r}, t)\rangle = 0$, we can write the linear response of the system as

$$\langle T(\vec{r}, t)\rangle = \frac{1}{k_B T} \sum_{\alpha} \lambda_{\alpha} \int_0^{\infty} d\tau \int d\vec{r}' \left\langle T(\vec{r}, 0) \sum_{i=1}^{N} \alpha_i \dot{\vec{r}}_i(\tau) \delta(\vec{r}_i(\tau) - \vec{r}') \right\rangle \cdot \vec{F}(\vec{r}', t-\tau). \tag{A4}$$

If we define a current density $\vec{g}^{\alpha}$ as

$$\vec{g}^{\alpha}(\vec{r}, t) = \sum_{i=1}^{N} \alpha_i \dot{\vec{r}}_i(t) \delta(\vec{r}_i(t) - \vec{r}), \tag{A5}$$

then (A4) may be rewritten as

$$\langle T(\vec{r}, t)\rangle = \frac{1}{k_B T} \sum_{\alpha} \lambda_{\alpha} \int_0^{\infty} d\tau \int d\vec{s} \langle T(\vec{0}, 0) \vec{g}^{\alpha}(\vec{s}, \tau)\rangle \cdot \vec{F}(\vec{r} + \vec{s}, t - \tau), \tag{A6}$$

where we have introduced the vectorial correlation function

$$\vec{G}^{T, g^{\alpha}}(\vec{s}, t) = (1/k_B T) \langle T(\vec{0}, 0) \vec{g}^{\alpha}(\vec{s}, t)\rangle. \tag{A7}$$

Equation (A6) is the required form of the response in space-time coordinates.

In our computations we were able to evaluate directly the quantity $\langle T(\vec{r}, t)\rangle$, obtaining in this way information on the collective modes of the system. Of course, (A7) is the corresponding response function from the knowledge of which $\langle T(\vec{r}, t)\rangle$ can also be calculated by linear response theory. Because of the convolution which appears on the right-hand side of (A6), it is useful to carry out both the analysis and the computations in terms of spatial Fourier transforms, denoting such a transform by a caret. We obtain successively

$$\hat{\vec{g}}^{\alpha}(\vec{k}, t) = V^{-1} \sum_{i=1}^{N} \alpha_i \dot{\vec{r}}_i(t) e^{-i\vec{k} \cdot \vec{r}_i(t)}, \tag{A8}$$

$$\hat{\vec{G}}^{T, g^{\alpha}}(\vec{k}, t) = V^{-1} \int d\vec{s}\, e^{-i\vec{k} \cdot \vec{s}} G^{T, g^{\alpha}}(\vec{s}, t), \tag{A9}$$

and

$$\langle \hat{T}(\vec{k}, t)\rangle = V \sum_{\alpha} \lambda_{\alpha} \int_0^{\infty} d\tau\, \hat{\vec{G}}^{T, g^{\alpha}}(-\vec{k}, \tau) \cdot \vec{F}(\vec{k}, t - \tau). \tag{A10}$$

From the translational invariance it follows that

$$\hat{\vec{G}}^{T, g^{\alpha}}(\vec{k}, t) = (1/k_B T) \langle \hat{T}(-\vec{k}, 0) \hat{\vec{g}}^{\alpha}(\vec{k}, t)\rangle, \tag{A11}$$

from which, finally, we obtain the result that

$$\langle \hat{T}(\vec{k}, t)\rangle = \frac{V}{k_B T} \sum_{\alpha} \lambda_{\alpha} \int_0^{\infty} d\tau \langle \hat{T}(\vec{k}, 0) \hat{\vec{g}}^{\alpha}(-\vec{k}, t)\rangle \cdot \hat{\vec{F}}(\vec{k}, t - \tau). \tag{A12}$$

If, in particular, the applied force is such that

$$\hat{\vec{F}}(k, t) = \hat{\vec{F}}_0(\vec{k}) \theta(t), \tag{A13}$$

the limiting mean value of $\hat{T}(\vec{k}, t)$ is given by

$$\langle \hat{T}(\vec{k}, \infty)\rangle = V \sum_{\alpha} \lambda_{\alpha} \int_0^{\infty} d\tau\, \hat{\vec{G}}^{T, g^{\alpha}}(-\vec{k}, \tau) \cdot \hat{\vec{F}}_0(\vec{k}). \tag{A14}$$

It is now very easy, choosing the appropriate dynamical variable and inserting it in (A12) or (A14), to find the corresponding formulas for the currents quoted in the text.

Let us now assume, for simplicity, that the external field is parallel to the $x$ direction. Then, because the electrical static conductivity $\sigma$ is simply the response in the optical longitudinal current to a longitudinal optical field, we obtain for $\sigma$ the expression

$$\sigma = \lim_{k, \omega \to 0} \sigma(\vec{k}, \omega) = e \hat{g}_x(0, \infty) / \hat{E}_{x,0}(0), \tag{A15}$$

or, using (A14),

$$\sigma = \frac{e^2 V}{k_B T} \int_0^{\infty} d\tau \langle \hat{g}_x(0, 0) \hat{g}_x(0, \tau)\rangle. \tag{A16}$$

Equation (A15) is equivalent to Eq. (9) of the main text, and Eq. (A16) is equivalent to Eq. (8).

From the phenomenological theory of shear viscosity we know that $\eta$ can be obtained from the acoustical current response to an acoustical transverse force field. To be more definite, let us assume that the vector field $\vec{F}(\vec{r}, t)$ has a component only in the $x$ direction and that this component is a function only of $z$. In the linear approx-

imation the current $\vec{J}^{\alpha}$ is given by

$$\hat{\vec{J}}^{\alpha}(\vec{k}, t) = \rho \hat{\vec{u}}^{\alpha}(\vec{k}, t), \quad \alpha = M, Q, \tag{A17}$$

where $\hat{\vec{u}}$ is the Fourier transform of the hydrodynamical velocity field. Then we can write[14] that

$$\eta = \lim_{k\to 0} \frac{\rho}{k^2} \frac{\hat{F}_{x,0}(k_z)}{\hat{u}_x^M(k_z, \infty)} = \lim_{k\to 0} \frac{\rho^2}{k^2} \frac{\hat{F}_{x,0}(k_z)}{\hat{J}_x^M(k_z, \infty)}. \tag{A18}$$

We can also express this result in terms of the appropriate response function of the system. Remembering that

$$\langle \hat{J}_x^M(k_z, t) \rangle = \frac{V}{k_B T} \int_0^{\infty} d\tau \, \langle \hat{g}_x^M(k_z, 0) \hat{g}_x^M(-k_z, \tau) \rangle \hat{F}_x(k_z)$$

$$= \int_0^{\infty} d\tau \, \hat{\sigma}_{xx}^{MM}(-k_z, \tau) \hat{F}_x(k_z), \tag{A19}$$

we obtain

$$\eta = \lim_{k\to 0} \frac{1}{k^2} \lim_{\omega\to 0} \frac{\rho^2}{\hat{\sigma}_{xx}^{MM}(-k_z, \omega)}$$

$$= \lim_{k\to 0} \frac{1}{k^2} \left(\frac{k_B T}{V}\right) \frac{\rho^2}{\int_0^{\infty} d\tau \, \langle \hat{g}_x^M(k_z, 0) \hat{g}_x^M(-k_z, \tau) \rangle}, \tag{A20}$$

where the limit $\omega \to 0$ has already been taken as a result of integrating over $\tau$.

---

*On leave of absence from Istituto di Matematica, Università di Camerino, Camerino, Italy.

[1]L. V. Woodcock and K. Singer, Trans. Faraday Soc. 67, 12 (1971).
[2]D. J. Adams and I. R. McDonald, J. Phys. C 7, 2761 (1974).
[3]J. W. E. Lewis, K. Singer, and L. V. Woodcock, J. Chem. Soc. Faraday Trans. 2 71, 308 (1975).
[4]M. P. Tosi and F. G. Fumi, J. Phys. Chem. Solids 25, 45 (1969).
[5]D. Levesque and L. Verlet, Phys. Rev. A 2, 2514 (1970).
[6]D. Levesque, L. Verlet, and J. Kurkijarvi, Phys. Rev. A 7, 1690 (1973).
[7]G. Jacucci and I. R. McDonald, Physica (to be published).
[8]J. P. Hansen and I. R. McDonald, J. Phys. C 7, L384 (1974); Phys. Rev. A 11, 2111 (1975).
[9]M. C. Abramo, M. Parrinello, and M. P. Tosi, J. Phys. C 7, 4201 (1974).
[10]G. Ciccotti and G. Jacucci, Report of Workshop on *Molecular dynamics of ionic systems*, Centre Européen de Calcul Atomique et Moléculaire, Orsay, France, 1975.
[11]J. P. Hansen, I. R. McDonald, and E. L. Pollock, Phys. Rev. A 11, 1025 (1975).
[12]S. G. Brush, H. L. Sahlin, and E. Teller, J. Chem. Phys. 45, 2102 (1966).
[13]R. Kubo, Rep. Prog. Phys. 29, 255 (1966).
[14]E. M. Gosling, I. R. McDonald, and K. Singer, Mol. Phys. 26, 1475 (1973).
[15]R. E. Young and J. P. O'Connell, Ind. Eng. Chem. Fundam. 10, 418 (1971).
[16]B. J. Alder, D. M. Gass, and T. E. Wainwright, J. Chem. Phys. 53, 3813 (1970).
[17]J. O'M. Bockris and N. E. Richards, Proc. R. Soc. A 241, 44 (1957).
[18]G. Jacucci, I. R. McDonald, and M. L. Klein, J. Phys. (Paris) 36, L97 (1975).
[19]J. L. Jackson and P. Mazur, Physica (Utr) 30, 2295 (1964).